

# Metal nanospheres under intense continuous wave illumination - a unique case of non-perturbative nonlinear nanophotonics

I. Gurwich, Y. Sivan\*

*Unit of Electro-optics Engineering, Faculty of Engineering Sciences,  
Ben-Gurion University of the Negev, Israel*

## Abstract

We show that the standard perturbative (i.e., cubic) description of the thermal nonlinear response of small metal nanospheres to intense continuous wave illumination is insufficient already beyond temperature rises of a few tens of degrees. In some cases, a cubic-quintic nonlinear response is sufficient to describe accurately the intensity dependence of the temperature, permittivity and field, while in other cases, a full non-perturbative description is required. We further analyze the relative importance of the various contributions to the thermal nonlinearity, identify a qualitative difference between Au and Ag, and show that the thermo-optical nonlinearity of the host typically plays a minor role, but its thermal conductivity is important.

---

\*Electronic address: sivanyon@bgu.ac.il

## I. INTRODUCTION

Nonlinear optical effects are usually considered weak. For example, typical second-order nonlinear processes such as second harmonic generation have efficiencies of a few percent for nonlinear crystals a few mm in length [1]. Third-order nonlinear effects are usually weaker and occur on even longer distances, see for example, self-phase modulation in optical fibers [2] or even in highly nonlinear semiconductor waveguides [3]. Accordingly, the vast majority of theoretical studies of nonlinear optical effects are performed within the framework of a perturbative description, i.e., involving, at most, a third-order (equivalently, cubic) nonlinearity.

Ultrafast nonlinearities are particularly weak. However, even the much stronger slow nonlinearities are limited to modest permittivity changes due to saturation effects (see [4] and references therein), phase transitions (e.g., in liquid crystals), or damage.

Here, we study a case, unique, to the best of our knowledge, whereby the perturbative description is insufficient, sometimes even requiring to go beyond a cubic-quintic nonlinearity to a full non-perturbative description. In particular, we consider a continuous wave (CW) illumination of a few nm metal sphere. We will focus on the *thermal* effect, known to be among the strongest sources of optical nonlinearity, with the dual aim of demonstrating the failure of the perturbative (cubic) description and identifying the importance of the various underlying physical effects. While doing so, we will elucidate the quantitative and qualitative differences between the strength of the thermal nonlinearity in the ultrafast and CW cases. This is important because while the former is well-studied, the latter, i.e., the CW case, has been practically ignored.

In that sense, this study was motivated by recent measurements of the extremely strong scattering of intense CW light from small metal particles [5–9], which, although being conceptually simple, are first of their kind. Further, this study was made possible by recent ellipsometry measurements of metal permittivities at elevated temperatures [10–13]. Thus, although we present here rather simple theoretical calculations, we emphasize that the approach is quite realistic. Indeed, it was already shown in [14] that the thermal effect reproduces *qualitatively* the experimental results of [5–9]. In the current article, we go beyond [14] and study this problem systematically and quantitatively, classifying the importance of the various contributing physical effects using numerical simulations and an approximate anal-

ysis. We identify qualitative differences between Au and Ag spheres, as well as between various hosts. This allows us to show that unless the host undergoes a phase transition (e.g., boiling), it has a relatively smaller role compared to the metal. Overall, all cases require a description beyond the standard perturbative description of the nonlinear response. In some cases, a cubic-quintic nonlinear response can capture the intensity dependence of the temperature, permittivity and field, while in other cases, a full non-perturbative description is required.

This study provides an important step towards reaching a quantitative understanding of the nonlinear scattering observed in [5–9] (i.e., matching theoretical predictions to the experimental data). It also allows us to predict so far unobserved behaviour, so that if observed experimentally, further support to the claims of the dominance of the thermal effects will be obtained.

The paper is organized as follows. In Section II, we describe the basic assumptions of the model, and in Section III we develop the model equations for the temperature, permittivity and field within the nanosphere. We then proceed by several numerical examples (Section IV) and complement the numerical results with an approximate analysis (Section V). Section VI provides a discussion of the results and an outlook.

## II. MODEL ASSUMPTIONS

In what follows, we denote the quantities within the metal nanosphere (host) with a subscript  $m$  ( $h$ ), and label the ambient properties by a 0 superscript.

We consider spheres which are sufficiently small so that the field and temperature within the metal nanosphere ( $E_m$  and  $T_m$ , respectively) are approximated as being uniform. The former assumption, known as the quasi-static approximation, is justified for particles sufficiently small with respect to the wavelength; the latter is valid when the host has a relatively lower thermal conductivity compared with the sphere (i.e.,  $\kappa_h \ll \kappa_m$ ).

We assume that the nanospheres exhibit only linear (one-photon) absorption. While we do not expect multi-photon absorption to yield anything more than a quantitative change to the results shown below, it is also worth noting that the absorption cross-sections of multi-photon processes are difficult to distinguish from the many other effects (e.g., the thermal effect, free-carrier generation, stress/strain etc.), and are in general not well characterized,

hence, difficult to quantify at this stage.

Further, we assume a linear dependence of the permittivity on the temperature, namely,

$$\epsilon_m(T) = \epsilon'_{m,0} + \left. \frac{d\epsilon'_m}{dT} \right|_{T_h^0} (T - T_h^0) + i \left( \epsilon''_{m,0} + \left. \frac{d\epsilon''_m}{dT} \right|_{T_h^0} (T - T_h^0) \right), \quad (1)$$

where  $T_h^0$  is the temperature of the host away from the nanosphere. This was shown to be the case at least up to several hundreds of degrees in recent ellipsometry measurements of Au [12, 13] thin films; the data in these studies was remarkably similar and was in excellent agreement with an earlier study [10] performed over a narrower temperature range. Similar behaviour was also seen for a Ag film [11], which describes probably the most detailed study, to date, of the temperature dependence of the Ag permittivity (in terms of wavelength and temperature range); it also includes an attempt to eliminate the effects of roughness, and is complemented with a first-principles calculation of the permittivity. It should be noted, however, that in contrast to the case of Au, the Ag results of [11] were not always in agreement with earlier studies; the authors of [11] included a detailed comparison and a discussion of the possible reasons for these differences. The most probable reason is the relatively large grain size, and the potential modification of the metal volume morphology at high temperatures, during and after the measurement themselves, see corresponding discussion in [12, 13].

Similarly, we assume for the host media that  $\epsilon_h = \epsilon'_{h,0} + d\epsilon'_h/dT|_{T_h^0}(T - T_h^0)$ . Finally, we assume that the thermal conductivity also varies linearly with temperature, i.e.,  $\kappa_h = \kappa_{h,0} + d\kappa_h/dT|_{T_h^0}(T - T_h^0)$ . Under the current conditions, the thermal conductivity can also account for the temperature dependence of the Kapitza resistance via a slight modification of the solution adopted here (see Eq. (2) below) [14, 15].

For brevity, in what follows, we denote  $B_m \equiv d\epsilon_m/dT|_{T_h^0} = B'_m + iB''_m$ ,  $B'_h = d\epsilon'_h/dT|_{T_h^0}$  and  $B_{\kappa,h} \equiv d\kappa_h/dT|_{T_h^0}$ . For simplicity, we consider hosts which exhibit negligible absorption ( $B''_h = 0$ ), however, any non-zero contribution will cause only a quantitative difference.

### III. MODEL

We showed in [14] that the temperature inside a few nm sphere under intense monochromatic illumination is uniform, and given by

$$\Delta T \equiv T_m - T_h^0 = \frac{a^2}{3\kappa_h(T)} p_{abs}(T), \quad p_{abs}(T) \equiv \frac{\omega}{2} \epsilon_0 \epsilon''_m(T) \left| \vec{E}_m \right|^2, \quad (2)$$

where  $a$  is the sphere radius,  $\omega$  is the angular frequency of the incoming photons,  $\epsilon_0$  is the vacuum permittivity, and where

$$\vec{E}_m = \frac{3\epsilon_h(T)}{\epsilon'_{tot}(T) + i\epsilon''_m(T)} \vec{E}_{inc}, \quad (3)$$

is the field inside the nanosphere,  $\vec{E}_{inc}$  is the incident field amplitude, and  $\epsilon'_{tot}(T) \equiv 2\epsilon_h(T) + \epsilon'_m(T)$ .

With the assumptions above, Eqs. (2)-(3) reduce to a 4-th order polynomial equation in  $\Delta T$ , namely,

$$\begin{aligned} & \underbrace{\frac{B_{\kappa,h}}{\kappa_{h,0}} \frac{B'_{tot}{}^2 + B_m''{}^2}{\epsilon''_{m,0}{}^2}}_{a_4} \Delta T^4 + \underbrace{\left[ \frac{B'_{tot}{}^2 + B_m''{}^2}{\epsilon''_{m,0}{}^2} + 2 \frac{B_{\kappa,h}}{\kappa_{h,0}} \frac{B'_{tot} \epsilon'_{tot} B_m'' \epsilon''_{m,0}}{\epsilon''_{m,0}{}^2} - \Delta T_{lin}^{on} \frac{B_h'^2 B_m''}{\epsilon_{h,0}'^2 \epsilon''_{m,0}} \right]}_{a_3} \Delta T^3 \\ & + \underbrace{\left[ 2 \frac{B'_{tot} \epsilon'_{tot} + B_m'' \epsilon''_{m,0}}{\epsilon''_{m,0}{}^2} + \frac{B_{\kappa,h}}{\kappa_{h,0}} \left( 1 + \frac{\epsilon'_{tot}{}^2}{\epsilon''_{m,0}{}^2} \right) - \Delta T_{lin}^{on} \left( 2 \frac{B_h'}{\epsilon_{h,0}'} \frac{B_m''}{\epsilon''_{m,0}} + \frac{B_h'^2}{\epsilon_{h,0}'^2} \right) \right]}_{a_2} \Delta T^2 \\ & + \underbrace{\left[ \left( 1 + \frac{\epsilon'_{tot}{}^2}{\epsilon''_{m,0}{}^2} \right) - \Delta T_{lin}^{on} \left( \frac{B_m''}{\epsilon''_{m,0}} + 2 \frac{B_h'}{\epsilon_{h,0}'} \right) \right]}_{a_1} \Delta T = \Delta T_{lin}^{on}, \end{aligned} \quad (4)$$

where  $B'_{tot} \equiv B'_m + 2B'_h$  and

$$\Delta T_{lin}^{on} \equiv \frac{3a^2 \omega \epsilon_0 \epsilon_{h,0}'^2 |\vec{E}_{inc}|^2}{2\kappa_{h,0} \epsilon''_{m,0}} = \frac{3a^2 \omega n_{h,0}^3 I_{inc}}{4c \kappa_{h,0} \epsilon''_{m,0}} > 0, \quad (5)$$

is the temperature rise in the on-resonance linear case [39] (see below) and where  $I_{inc} = 2\sqrt{\epsilon_{h,0}'} |\vec{E}_{inc}|^2 / Z_0$  is the incident intensity. More generally,  $\Delta T_{lin}^{on}$  is proportional to  $P_{abs}$ , the density of power absorbed within the sphere, namely,  $\Delta T_{lin}^{on} = P_{abs} / 4\pi \kappa_{h,0} a$  [16]. Eq. (5) shows that under the quasistatic approximation used here, a change of the nanosphere radius or thermal conductivity of the host is equivalent to a rescaling of the incident intensity.

We note that all the coefficients in Eq. (4) involve only the ratios of a thermo-derivatives of the respective parts of the permittivities and the permittivities themselves ( $\epsilon''_{m,0}$  or  $\epsilon'_{h,0}$ ).

It is clear that one can distinguish between two generic scenarios - when the illumination is on-resonance ( $\epsilon'_{tot} \ll \epsilon''_{m,0}$ ) or off-resonance (otherwise). We showed in [14] that there is a qualitative difference between these two cases, something which can, in fact, be observed from the solution of the linear case (i.e., the solution of Eq. (4) where all the thermo-derivatives vanish),

$$\Delta T_{lin} = \frac{\epsilon''_{m,0}{}^2}{\epsilon''_{m,0}{}^2 + \epsilon'_{tot}{}^2} \Delta T_{lin}^{on}. \quad (6)$$

Indeed, Eq. (5) shows that in the off-resonance case, the temperature rise is higher for increasing  $\epsilon''_{m,0}$ , while the opposite is true for the on-resonance case.

With the solution for the temperature in hand, the permittivity is given by Eq. (1) and the field within the nanosphere by Eq. (3). Specifically,

$$\begin{aligned}\vec{E}_m(\Delta T(E_{inc})) &= \frac{3(\epsilon'_{h,0} + B'_h \Delta T)}{\epsilon'_{tot} + B'_{tot} \Delta T + i\epsilon''_{m,0} + iB''_m \Delta T} \vec{E}_{inc} \\ &= \frac{3\epsilon'_{h,0}}{\epsilon'_{tot} + i\epsilon''_{m,0}} \left( \frac{1 + \frac{B'_h \Delta T}{\epsilon'_{h,0}}}{1 + \frac{B'_{tot} + iB''_m \Delta T}{\epsilon'_{tot} + i\epsilon''_{m,0}}} \right) \vec{E}_{inc},\end{aligned}\quad (7)$$

where [17, 18]

$$f \equiv 3\epsilon'_{h,0}/(\epsilon'_{tot} + i\epsilon''_{m,0}), \quad (8)$$

is the usual Figure of Merit for field enhancement inside a nanosphere [17], sometimes referred to as the Faraday number [19]. At resonance, this reduces to

$$\begin{aligned}\vec{E}_m(\Delta T(E_{inc})) &= \frac{3\epsilon'_{h,0}}{i\epsilon''_{m,0}} \frac{1 + \frac{B'_h \Delta T}{\epsilon'_{h,0}}}{1 + \left( \frac{B''_m}{\epsilon''_{m,0}} - i\frac{B'_{tot}}{\epsilon''_{m,0}} \right) \Delta T} \vec{E}_{inc} \\ &\cong \frac{3\epsilon'_{h,0}}{i\epsilon''_{m,0}} \left( 1 + \frac{B'_h \Delta T}{\epsilon'_{h,0}} \right) \left( 1 - \left( \frac{B''_m}{\epsilon''_{m,0}} - i\frac{B'_{tot}}{\epsilon''_{m,0}} \right) \Delta T \right) \vec{E}_{inc} \\ &\cong -if^{(res)} \left[ 1 - \left( \frac{B''_m}{\epsilon''_{m,0}} - \frac{B'_h}{\epsilon'_{h,0}} - i\frac{B'_{tot}}{\epsilon''_{m,0}} \right) \Delta T \right] \vec{E}_{inc} \\ &= \left[ 1 - \left( \frac{B''_m}{\epsilon''_{m,0}} - \frac{B'_h}{\epsilon'_{h,0}} - i\frac{B'_{tot}}{\epsilon''_{m,0}} \right) \Delta T \right] \vec{E}_m(T = T_h^0),\end{aligned}\quad (9)$$

where  $f^{(res)} \equiv 3\epsilon'_{h,0}/\epsilon''_{m,0}$ . Note that we expanded the denominator to first order accuracy in  $\Delta T$ , the accuracy level of Eq. (1).

If the intensity is low, then  $\Delta T \rightarrow \Delta T_{lin}$ . In this case, Eqs. (5)-(6) provide the perturbative description of the thermal nonlinearity of metals (as a cubic nonlinearity), where  $\chi_m^{(3)} |\vec{E}_m|^2 \sim B_m \Delta T_{lin}$  [18]. Any deviation from this solution, specifically, employing higher intensities, or due to a deviation from the linear dependence of the coefficients on the parameters will give rise to a deviation from the standard perturbative description of a cubic nonlinear response. While this may not be a new or surprising observation, unlike the well-studied ultrafast nonlinearity, the CW nonlinearity of metals in general, and of a single metal nanosphere, in particular, was not studied systematically at all. Accordingly, we aim

here to study this case in detail and to show that the perturbative (cubic) description is insufficient in a wide range of configurations.

Specifically, we will solve Eq. (4) and compute the permittivity (1) and field (3) for a varying level of illumination. Despite its considerable simplicity, the analytical solution of Eq. (4) is too complicated for meaningful physical analysis. Accordingly, we proceed by a numerical solution of Eq. (4). In all the examples below, we will limit ourselves to a maximal temperature rise of  $\Delta T \approx 300^\circ K \sim T_h^0$ , a range in which the assumptions detailed above should hold [12]. In this range, one avoids sintering and melting of the metal [20] as well as damage to the host. The quantitative discussion below will refer to the values obtained at the maximal incoming intensity.

We focus on Au and Ag, for which the temperature dependence of the permittivity was recently characterized [10–13]. We consider generic dielectric hosts such as an index matching oil and a (solid) semiconductor. Additional material choices can be analyzed along the same lines. Note we avoid water as a host in order to avoid complications associated with the limited range of temperature increase before boiling, super heating and bubble formation [21–23]. Our wavelength choices are rather customary, so that overall, the examples below are fairly generic.

## IV. NUMERICAL EXAMPLES

### A. Au nanospheres in a liquid host

We set  $\lambda = 550\text{nm}$  such that  $\epsilon_{Au,0} = -5.3 + 1.76i$  and  $B_{Au} = (0.7 + 1.7i) \cdot 10^{-3}/^\circ K$  [13] so that with a liquid host for which  $\epsilon_h = 2.65$ , the illumination is resonant. We also set  $\kappa_{h,0} = 0.15 \text{ W/m}/^\circ K$  and  $B'_h = 10^{-4}/^\circ K$  [24]; these three parameters correspond to an index matching oil, used in the experiments of [5–9]. In the absence of concrete data, we estimate  $B_{\kappa,h} = 5 \cdot 10^{-5} \text{ W/m}/^\circ K^2$  such that  $B_{\kappa,h}/\kappa_{h,0} \sim 3 \cdot 10^{-4}/^\circ K$ , and at  $\Delta T = 300^\circ K$ , the change of  $\kappa_h$  is  $\sim 10\%$ .

Fig. 1(a) shows that the temperature grows monotonically with the incoming intensity, but with a decreasing slope; we refer to this behaviour as a “saturation” of the thermal response. The deviation of the solution of the 4-th order polynomial (4) from the standard linear solution (5), i.e., the solution of Eq. (4) with  $a_2 = a_3 = a_4 = 0$ , reaches several tens

of percent. However, this deviation decreases to less than 10% and even less than 0.5% if the second order (i.e., with  $a_2 \neq 0$ ) and third order ( $a_2, a_3 \neq 0$ ) terms, respectively, are accounted for. The addition of the fourth-order term (i.e., also with  $a_4 \neq 0$ ) has a very small effect.

Figs. 1(b)-(c) show the changes of the real and imaginary parts of the Au permittivity, respectively. The relative change of  $\epsilon'_{Au}$  is a few percent, but the relative change of  $\epsilon''_{Au}$  is  $\sim 26\%$ . Figs. 1(b)-(c) also show the fit to the exact solution of Eq. (4), with either a first- or second-order polynomial in the incoming intensity, corresponding to a cubic or cubic-quintic approximation of the nonlinear response, respectively [40]. As seen, *the cubic fit provides a good match to the exact results only up to a temperature rise of a few tens of degrees*, so that the standard perturbative (cubic) description is inadequate. Instead, the cubic-quintic fit provides a decent match to the exact solution within the current temperature range, reflecting the “saturation” of the thermal effect, or equivalently, the decrease of the quality factor of the plasmonic resonator.

Finally, Fig. 1(d) shows the field within the nanosphere. As expected, it decreases due to the increase of the imaginary part of the permittivity. Again, while the cubic fit is accurate only for a limited range of temperatures (hence, intensities), the cubic-quintic fit provides quite a satisfactory fit of the exact numerical results.

Since  $B'_{tot}\Delta T = O(10^{-1}) \ll \epsilon''_{Au,0}$  for the temperature rise of  $O(100^\circ K)$  studied here, we see that typically, the changes of the field due to the changes of the real part of the Au permittivity, corresponding to a spectral shift of the resonance position, are smaller than those incurred by the changes to the imaginary part. In other words, the fact that the plasmonic resonance is typically broad, and the relative larger magnitude of  $B''_{Au}$ , make the system relatively less sensitive to changes of the real part of the Au permittivity. As shown below, this conclusion does not apply to Ag nanospheres. In that regard, a direct test of the importance of  $B'_m$  and  $B'_h$  shows that their neglect leads to a maximal error smaller than 1% ( $\sim 3^\circ K$ ) in the temperature rise (with respect to a  $\sim 100\%$  total change of  $\sim 300^\circ K$ ) [41]. However, neglecting  $B_{\kappa,h}/\kappa_{h,0}$  leads to a relative error of  $\sim 7\%$  for the temperature rise [42]. As shown below, this occurs because to leading order,  $B_{\kappa,h}/\kappa_{h,0}$ , affect the temperature rise on the same order as  $B''_m/\epsilon''_{m,0}$ , so that it is more influential compared to the other thermo-derivatives.



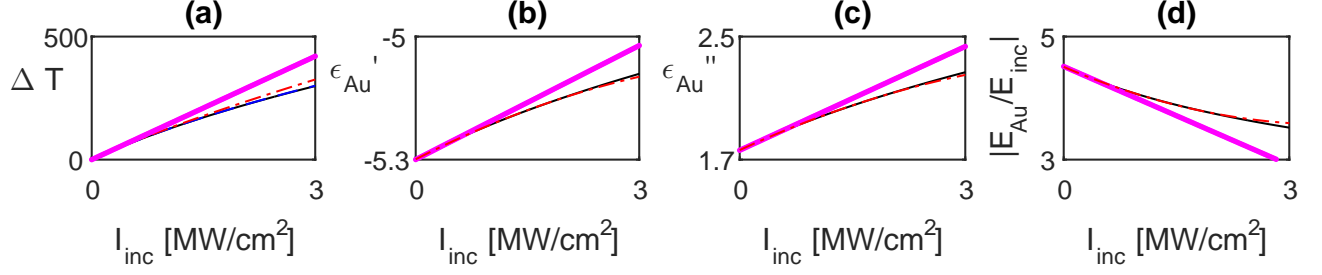


FIG. 1: (Color online) (a) The temperature rise (i.e.,  $\Delta T$ , the solution of Eq. (4); black solid line) inside a Au sphere in a liquid host ( $\epsilon_h = 2.65$ ) illuminated at  $\lambda = 550\text{nm}$  as a function of the incident intensity. The solutions accounting for up to third/second/first order terms are shown by blue dashed/red dash-dotted/magenta dotted lines, respectively; however, in the current case, the black and blue lines are essentially indistinguishable. (b) Real and (c) imaginary parts of the Au permittivity as a function of the incoming intensity, based on the exact solution of Eq. (4) (black solid line) compared with its cubic approximation (red dash-dotted line) and a cubic-quintic approximation (magenta dotted line). (d) Same as (b)-(c) for the normalized electric field within the nanosphere.

## B. Au nanospheres in a AlGaAs host

We now choose a solid host, specifically,  $\text{Al}_x\text{Ga}_{1-x}\text{As}$  with  $x = 30\%$  Al content, such that the host is transparent up to the visible spectral range, and exhibits a rather high permittivity of  $\sim 13$  near the band edge (i.e., about 5 times higher than the oil liquid employed above). Accordingly, the localized plasmon resonance occurs at  $\lambda = 800\text{nm}$  where  $\epsilon_{Au,0} = -26.5 + 2i$  [12]; in addition,  $B_{Au} = (2 + 2.6i) \cdot 10^{-3}/^\circ K$  which corresponds to the largest value of  $B''_{Au}/\epsilon''_{Au,0}$  in the optical spectral domain.

This choice of Al content also corresponds to nearly minimal value of thermal conductivity,  $\kappa_{h,0} \approx 13 \text{ W/m}/^\circ K$  [25], i.e., about 100 times higher than for oil, but still about 20 times smaller than for metals. Thus, the error associated with neglecting the temperature non-uniformity amounts to no more than 2% [14]. This error is much smaller than all the effects demonstrated below.

Based on data for GaAs [26], we estimate  $B'_{AlGaAs} \approx 2 \cdot 10^{-3}/^\circ K$  (such that

$B'_{AlGaAs}/\epsilon'_{AlGaAs,0} \sim 10^{-4}/^{\circ}K$ ; this is similar to the liquid, and about an order of magnitude smaller than the corresponding ratio for metals [43]) and estimate  $B_{\kappa,h} = 5 \cdot 10^{-4} W/m/^{\circ}K^2$  such that at  $\Delta T = 300^{\circ}K$ , the change of  $\kappa_h$  is  $\sim 1\%$ , i.e., it is negligible. We ignore strain/stress that may develop within the solid host due to the heating. These effects may only increase the nonlinear response.

Fig. 2 shows results which are qualitatively similar to the case of liquid host (Fig. 1), however, for  $\Delta T_{lin}^{on}$  which is 13 times smaller. This shows, in contrast to what one may expect based on the ultrafast case (see, e.g., [17, 19], Eqs. (7)-(9) and discussion below), that the metal-semiconductor system is *less* nonlinear than the metal-liquid system. This is a direct result of the heat diffusion in the host, and more generally, of the spatially non-local nature of the thermal nonlinearity in the system, causing lower effective heating of the metal nanosphere.

Another striking difference between Fig. 1 and Fig. 2 is that in the latter, neither the cubic nor the cubic-quintic fits provide a good match to the exact variations of the permittivity and field. As will be shown below, this can be traced to the relatively larger value of the (relative) change of the real part of the metal permittivity.

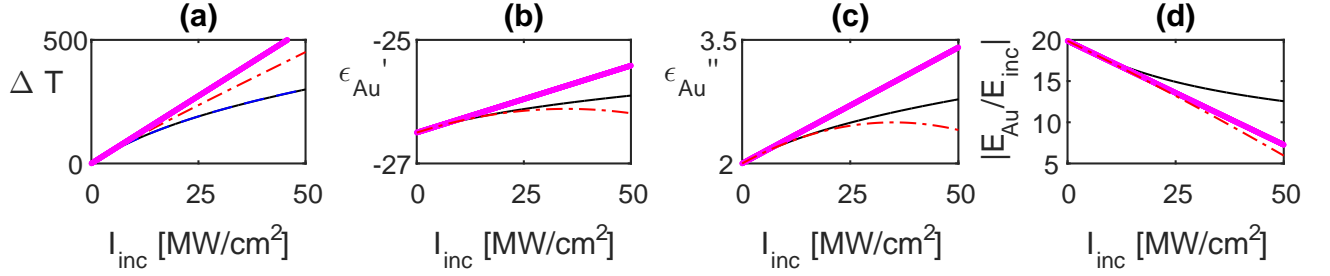


FIG. 2: (Color online) Same as Fig. 1 for a  $Al_{0.3}Ga_{0.7}As$  host with  $\lambda = 800nm$  and  $\epsilon_h = 13$ .

### C. Ag nanospheres in a liquid host

We now replace the Au spheres with Ag spheres and set  $\lambda = 450nm$  such that  $\epsilon_{Ag,0} = -4.7 + 1.55i$  and  $B_{Ag} = (-46 + 2.5i) \cdot 10^{-4}/^{\circ}K$  [11]. Note that at this wavelength, the thermo-derivative of the real part of the metal permittivity is 7 times higher than Au, and

has the opposite sign; in addition, the thermo-derivative of the imaginary part is much smaller than in previous examples.

The temperature rise shown in Fig. 3(a) is reminiscent to those shown above, however, in contrast to previous cases, the real part of the permittivity of the Ag particle decreases (rather than increases). More importantly, although Fig. 3(d) shows results which look quantitatively similar to the cases of Au particles, the reason for the decrease of scattering for the Ag particles is different - it originates from the change of the real part of the permittivity rather than the change of the imaginary part, i.e., the field decreases due to a shift *away from resonance*, rather than due to a decrease of the quality factor of the resonator. Indeed, the change of the real part (Fig. 3(b)) is far larger than the change of the imaginary part (Fig. 3(c)). This dominance also makes the cubic-quintic fit quite satisfactory, in contrast to what is seen in Fig. 2.

This observation prompts us to predict the opposite behaviour, so far not observed experimentally. Specifically, if the illumination is initially non-resonant, the heat generation can cause the system to shift *into* resonance, hence, the quality factor and local field amplitude to increase. This is shown in Fig. 4. Peculiarly, this example shows a deviation from the perturbative description in (a), yet, (b)-(d) are well described by a cubic-quintic nonlinearity.

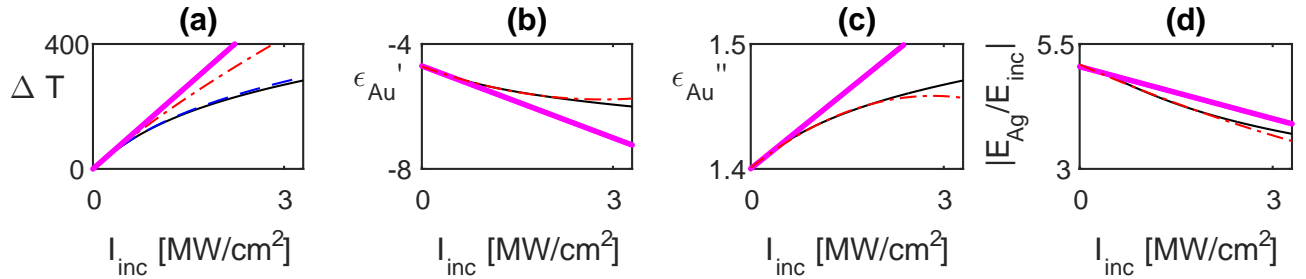


FIG. 3: (Color online) Same as Fig. 1 with Ag nanospheres and  $\lambda = 450\text{nm}$  and  $\epsilon_h = 2.35$ .

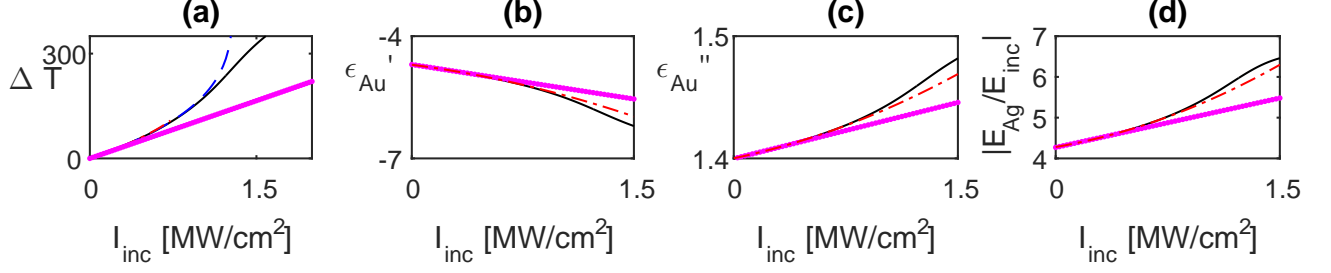


FIG. 4: (Color online) Same as Fig. 3 with  $\epsilon_h = 3.25$ .

## V. MORE ANALYSIS AND SIMPLIFICATION

We now try to simplify Eq. (4) by identifying the leading order terms, in order to complement the numerical solutions shown above with an approximate analysis, valid for the moderately high intensity range. This is especially important in order to emphasize the deviation from the perturbative description of the nonlinear response and to elucidate the relative importance of the various physical effects and how each of them affects the temperature, permittivity and field.

The easiest way to obtain analytical insights is, as already done in the numerical simulations above (see red lines in Figs. 1(a) & 2(a)), to limit ourselves to small intensities, hence, to a small temperature rise, such that it is justified to keep only the terms up to the second order of  $\Delta T$  in Eq. (4), i.e., to set  $a_3 = a_4 = 0$ . In this case,

$$\Delta T = \frac{a_1}{2a_2} \left( \sqrt{1 + 4 \frac{a_2}{a_1^2} \Delta T_{lin}^{on}} - 1 \right). \quad (10)$$

This shows that in general, the temperature rise does not scale linearly with the incoming intensity (via  $\Delta T_{lin}$  (6)) as one would expect from the perturbative description; instead, it follows a square-root law, i.e., it grows more slowly (for  $a_2 > 0$ , which is the usual case, see discussion below); we referred to this behaviour as a “saturation” of the thermal effect. This is in agreement with the numerical results shown above.

For even smaller intensities, we can expand the square root in a Taylor series [44] such that

$$\Delta T = \frac{\Delta T_{lin}^{on}}{a_1} - \frac{a_2}{a_1^3} (\Delta T_{lin}^{on})^2 + \dots, \quad (11)$$

where  $\Delta T_{lin}^{on}$  (5) scales with  $I_{inc}$ ,  $a^2$ , and  $\kappa_{h,0}^{-1}$ ; similarly, the nonlinear correction to the temperature scales with  $I_{inc}^2$ ,  $a^4$ , and  $\kappa_{h,0}^{-2}$ .

Eqs. (1), (4) and (11) show that the relative importance of a specific physical effect (i.e., a specific thermo-derivative) is related to the highest order coefficient of (4) it appears in, e.g., the cubic term depends on  $a_1$ , the quintic depends also on  $a_2$  etc.. Specifically, this shows that  $B_{\kappa,h}/\kappa_{h,0}$  affects the temperature rise and field (7) only via the quintic term.

We also note, however, that some of the contributions to the coefficients  $a_1$  to  $a_3$  are proportional to  $\Delta T_{lin}^{on}$ . These will, naturally, contribute only to the next order in  $\Delta T_{lin}^{on}$  (or equivalently, in  $I_{inc}$ ). Specifically, this shows that although  $B'_h$  appears in  $a_1$ , it too affects the temperature rise  $\Delta T$  only via the quintic term. Note that somewhat unintuitively, this is lower than its effect on the field (3).

Further distinction between the various contributions can be attained by noting that typically, the permittivity of a (host) *dielectric* material is less sensitive to temperature than the metal, i.e.,

$$B'_h/\epsilon'_{h,0} \ll |B'_m/\epsilon''_{m,0}|, |B'_m/\epsilon'_{m,0}|, |B''_m/\epsilon''_{m,0}|. \quad (12)$$

Indeed, one can compare e.g., recent ellipsometry results [11–13] with values detailed in [1]; see also specific examples above [45]. Accordingly, although it appears in the quintic term, the contribution of  $B'_h$  to the temperature rise  $\Delta T$  is small relative to  $B''_m$  such that it affects  $\Delta T$  only for very high incoming intensities, beyond the cubic-quintic description. Again, this is lower than its effect on the field (3).

Even further distinction can be made for a specific spectral configuration. At resonance, i.e., for  $\epsilon''_{m,0} \gg \epsilon'_{tot} \rightarrow 0$ , Eq. (4) reduces to

$$\underbrace{\left[ 2\frac{B''_m}{\epsilon''_{m,0}} + \frac{B_{\kappa,h}}{\kappa_{h,0}} - \Delta T_{lin}^{on} \left( 2\frac{B''_m B'_h}{\epsilon''_{m,0} \epsilon'_{h,0}} + \frac{B'^2_h}{\epsilon'^2_{h,0}} \right) \right]}_{a_2} \Delta T^2 + \underbrace{\left[ 1 - \Delta T_{lin}^{on} \left( \frac{B''_m}{\epsilon''_{m,0}} + 2\frac{B'_h}{\epsilon'_{h,0}} \right) \right]}_{a_1} \Delta T = \Delta T_{lin}^{on}. \quad (13)$$

Organizing the orders of  $\Delta T_{lin}^{on}$ , Eq. (11) reduces to

$$\Delta T = \Delta T_{lin}^{on} - \left( \frac{B''_m}{\epsilon''_{m,0}} + \frac{B_{\kappa,h}}{\kappa_{h,0}} + 2\frac{B'_h}{\epsilon'_{h,0}} \right) (\Delta T_{lin}^{on})^2 + \dots \quad (14)$$

Thus, the thermo-derivatives affect the temperature rise  $\Delta T$  via the quintic or higher order terms. Note that the various terms may not necessarily have the same sign, so that they can balance each other. However, by Eq. (12),  $B'_h/\epsilon'_{h,0}$ , is typically smaller with respect to  $B''_m/\epsilon''_{m,0}$ , so that the sign of  $B'_h$  is of lesser importance and the quintic coefficient can

be simplified. In addition, Eq. (14) shows that in this case,  $B'_m$  appears only beyond the quintic-order. These two facts a-posteriori justify the numerical results shown in [14] and in Section IV A.

In addition, Eq. (14) explains the failure of the cubic-quintic fit in the Au-AlGaAs case (Section IV B and Fig. 2). Indeed, in this case, the relative larger value taken by  $B'_{Au}$  makes the  $a_3$  term in Eq. (4) relatively more important than in the liquid host case, hence, it gives rise to a deviation from the cubic-(quintic) description.

However, Eq. (14), which does not account for  $B'_m$ , fails to reproduce the results of Figs. 3-4 where the contributions of  $B_{\kappa,h}$  and  $B''_m$  are relatively small. Indeed, in these cases, the  $a_3$  and  $a_4$  terms of Eq. (4) are of comparable magnitude to that of the  $a_2$  term already for a small temperature rise and the approximation (10) is not valid anymore.

Away from resonance, i.e., for  $\epsilon'_{tot} \gg \epsilon''_{m,0}$ , Eq. (11) can be approximated by

$$\Delta T \approx \left( \frac{\epsilon''_{m,0}}{\epsilon'_{tot}} \right)^2 \Delta T_{lin}^{on} - \left( \frac{B''_m}{\epsilon''_{m,0}} + 2 \frac{B'_h}{\epsilon'_{h,0}} + \left[ 2 \frac{B'_{tot} \epsilon'_{tot}}{\epsilon''_{m,0}^2} + \frac{B_{\kappa,h}}{\kappa_{h,0}} \left( \frac{\epsilon''_{m,0}}{\epsilon'_{tot}} \right)^{-2} \right] \left( \frac{\epsilon''_{m,0}}{\epsilon'_{tot}} \right)^6 \right) (\Delta T_{lin}^{on})^2 + \dots \quad (15)$$

Thus, with respect to the on-resonance case, the cubic term is smaller and for the quintic case, the weights of the various thermo-derivatives are different. Specifically, the quintic term now includes also  $B'_m$ . This explains the relatively larger role played by  $B'_{Ag}$  in Figs. 3 and 4 compared to all other examples. Eq. (15) would be also relevant to thin films (assuming no means for phase matching is adopted).

## VI. DISCUSSION

The numerical examples and consequent approximate analysis above show that the non-linear thermal response is cubic only for a modest temperature rise of a few tens of degrees; this is a regime where the nonlinear response is, in fact, frequently ignored altogether [16]. Beyond this range, a cubic-quintic nonlinear response is sufficient in cases where either  $B'_m$  or  $B''_m$  dominate all other thermo-derivatives. Otherwise, a fully non-perturbative description of the thermal response is required.

Overall, the changes of the metal permittivity dominate the nonlinear thermal response of the nanosphere configuration. However, this does not mean that the effects of thermal lensing due to heating of the host are secondary. Indeed, the host occupies, in general, a

much larger fraction of space; their role should anyhow be studied in the context of effective medium theory, which is beyond the scope of the current study.

We note that all the cases studied here involved  $B_m'' > 0$ , leading typically to the “thermal saturation” described above - the temperature grows more slowly at high intensities compared to low intensities. In turn, this leads to a decrease of the internal and scattered fields with increasing intensity [14]. This behaviour was indeed observed in all experiments of nonlinear scattering from metal nanoparticles under CW illumination performed so far [5–9][46]. However, the ellipsometry data reveals narrow spectral regimes where  $B_m'' < 0$ , e.g., for Au for  $\lambda < 500\text{nm}$  (due to the effect of the Fermi smearing on the interband transitions [27, 28]). This regime is, however, out of the resonance band, hence, the response of the system is expected to be weak in this regime. For Ag [11], a much narrower regime in which  $B_m'' < 0$  around  $\lambda = 400\text{nm}$  was identified. Even then, the thermo-derivatives in this regime are much smaller than in the examples above. Yet, although elusive, such a regime is clearly highly desirable for plasmonic applications, since it gives rise to higher quality factors and *stronger* fields. We emphasize, however, that this effect should not be confused with saturable absorption (= partial population inversion, thus, associated with a non-thermal electron distribution), which could explain the intriguing “reverse saturable” scattering observed in [5–8][47].

It is tempting to write the temperature dependent term in Eq. (1) as the product of the intensity and the cubic nonlinear coefficient associated with the thermal effect, and similarly for the quintic effect etc.. However, strictly speaking, such as expansion (1) *cannot* be regarded as an inherent material parameter, because although it involves the intrinsic material electromagnetic response of the metal, it also involves, as would happen for any structure, the size of the nanosphere, and the electromagnetic and thermal response of the host[48]. On the other hand, the temperature-dependent term (1) cannot be understood as an effective nonlinearity either, since such a quantity necessarily involves the fill factor, inter-particle interactions etc..

Thus, the correction to the permittivity,  $B_m\Delta T$ , or its leading order term  $B_m\Delta T_{lin}$ , should be understood as a Figure of Merit (FOM) for the nonlinear response. Specifically, the values of nonlinear coefficients reported in [9] cannot be compared to other reported values of intrinsic nonlinearity of metals.

Note that our FOM,  $B_m\Delta T_{lin}$ , is proportional to the absorption cross-section of the

nanosphere or equivalently, to the Joule number [19]. It, however, includes also information about the absolute temperature rise for a given incoming intensity and host by accounting for heat diffusion in the host. Accordingly, while the conventional FOM (Eq. (8) and [17, 19]) is relevant globally for linear optics, in the context of intense illumination, it is useful only for ultrafast illumination where the thermal properties do not play an important role, i.e., when the response is spatially-local. In all other cases, especially the many associated applications, our FOM should be used. Specifically, our FOM shows that the highest thermal nonlinearity will be obtained for a dilute host (e.g., gas, or even vacuum), due to its low thermal conductivity.

The results of the current manuscript are specific to a few nm sphere. However, we believe that our claims apply also to larger spheres, as well as to particles of other shapes, with only quantitative differences associated with the non-uniformity of the field and temperature.

The results presented above and the good match to experimental results [14] support the interpretation of the experimental results of nonlinear scattering of CW light from the small nanospheres as a thermal nonlinear effect. However, many effects which do not play an important role in the ultrafast case, may have a non-negligible contribution in the CW case; these include specifically, stress/strain, partial population inversion due to interband transitions [18], free-carrier generation, multi-photon absorption etc.. In that regard, our study identifies several easy measurements that may allow us to establish the dominance of the thermal effect over all the additional ones.

First, we show that the variation of  $\kappa_h$ , which appears only in the thermo-optical nonlinearity studied here, may enable the isolation experimentally the role of the thermal effect. An attempt to do that was made in [29], however, this study ignored various additional relevant factors like the size of the particles that affects the leading order solution  $\Delta T_{lin}$  (6). It also compared composites with different densities (details not provided) that could also affect the effective response due to the long range nature of the thermal interactions between adjacent nanospheres. These facts can explain the large discrepancy in [29] between the theoretical prediction (based solely on the value of the thermal conductivity) and the experimental observations. A more accurate match requires accounting for all the additional parameters, including  $B_{\kappa,h}$  which appears on the quintic order (14), for size effects by relaxing the assumptions on field and temperature uniformity, as well as for the potential absorption in the host. Alternatively, one has to compare the measurement of a composite



to a full effective medium theory for a composite.

Second, the configuration described in Fig. 4 is related, again, with a unique signature of the thermal effect. However, we emphasize that there is still some uncertainty regarding the exact values of  $B_m$  for Ag, especially due to possible differences of morphology of particles made with different methods (see e.g., discussion in [13]).

Finally, although the most accessible experimental indication for nonlinear scattering is the far field intensity, there is growing interest in measuring temperature in the near field [30–35]. Such measurements will give the ultimate evidence regarding the role of the thermal effect. The formulation, numerical results and analysis described in this manuscript will provide valuable predictions for such measurements.

In this study, we limited ourselves to the thermal effects and modest temperature increases. Beyond that range, the thermo-derivatives are not necessarily constant, giving rise to further deviation from the perturbative description. In addition, other effects may become important for higher temperatures/intensities, e.g., multi-photon absorption, and non-thermal effects [49]. In the presence of the latter, one would not be able to use the high temperature ellipsometry results of [12, 13] which are relevant only for metals at thermal equilibrium, i.e., their electrons obey the Fermi-Dirac distribution. Clearly, at even higher temperatures, the metal would undergo sintering and eventually melting, and the host may get damaged.

As a final statement, this study provides an important step towards the characterization of the effective response of arrays of particles, which can be regarded as thermo-optical metamaterials - artificial materials that change their electromagnetic properties under laser illumination due to temperature rise. These would have to be studied under proper effective medium theory and beyond the perturbative description, accounting not only for the electromagnetic interactions between the nanoparticles, but also for the thermal interaction between them. The latter is expected to have a far longer length scale. This fact, together with the use of an absorptive nonlinearity, may allow surpassing the limitations detailed in [4] for highly nonlinear metamaterials.

---

[1] R. W. Boyd. *Nonlinear Optics*. Academic Press, 2nd edition, 2003.

[2] G. P. Agrawal. *Nonlinear Fiber Optics*. Academic Press, 3rd edition, 2001.

- [3] Q. Lin, O. J. Painter, and G. P. Agrawal. Nonlinear optical phenomena in silicon waveguides: modeling and applications. *Optics Express*, 15:16604, 2007.
- [4] J. B. Khurgin and G. Sun. Plasmonic enhancement of the third order nonlinear optical phenomena: Figures of merit. *Optics Express*, 21:27460–27480, 2013.
- [5] S.-W. Chu, H.-Y. Wu, Y.-T. Huang, T.-Y. Su, H. Lee, Y. Yonemaru, M. Yamanaka, R. Oketani, S. Kawata, and K. Fujita. Saturation and reverse saturation of scattering in a single plasmonic nanoparticle. *ACS Photonics*, 1:32–37, 2013.
- [6] S.-W. Chu, T.-Y. Su, R. Oketani, Y.-T. Huang, H.-Y. Wu, Y. Yonemaru, M. Yamanaka, H. Lee, G.-Y. Zhuo, M.-Y. Lee, S. Kawata, and K. Fujita. Measurement of a saturated emission of optical radiation from gold nanoparticles: Application to an ultrahigh resolution microscope. *Phys. Rev. Lett.*, 112:017402, 2014.
- [7] H. Lee, R. Oketani, Y.-T. Huang, K.-Y. Li, Y. Yonemaru, M. Yamanaka, S. Kawata, K. Fujita, and S.-W. Chu. Point spread function analysis with saturable and reverse saturable scattering. *Optics Express*, 22:26016–26022, 2014.
- [8] Y.-T. Chen, P.-H. Lee, P.-T. Shen, J. Launer, R. Oketani, K.-Y. Li, Y.-T. Huang, S. Shoji, S. Kawata, K. Fujita, and S.-W. Chu. Study of nonlinear plasmonic scattering in metallic nanoparticles. *ACS Photonics*, 3:1432–1439, 2016.
- [9] H.-Y. Wu, Y.-T. Huang, P.-T. Shen, H. Lee, R. Oketani, Y. Yonemaru, M. Yamanaka, S. Shoji, K.-H. Lin, C.-W. Chang, S. Kawata, K. Fujita, and S.-W. Chu. Ultrasmall all-optical plasmonic switch and its application to superresolution imaging. *Scientific Reports*, 6:24293, 2016.
- [10] R.B. Wilson, B.A. Apgar, L.W. Martin, and D.G. Cahill. Thermoreflectance of metal transducers for optical pump-probe studies of thermal properties. *Optics Express*, 20:28829 – 28838, 2012.
- [11] S. T. Sundari, S. Chandra, and A. K. Tyagi. Temperature dependent optical properties of silver from spectroscopic ellipsometry and density functional theory calculations. *J. Appl. Phys.*, 033515:114, 2013.
- [12] H. Reddy, U. Guler, A. V. Kildishev, A. Boltasseva, and V. M. Shalaev. Temperature-dependent optical properties of gold thin films. *Optical Materials Express*, 6:2776–2802, 2016.
- [13] P.-T. Shen, Y. Sivan, C.-W. Lin, H.-L. Liu, C.-W. Chang, and S.-W. Chu. Temperature- and -roughness dependent permittivity of annealed/unannealed gold films. *Optics Express*, 24:19254, 2016.

- [14] Y. Sivan and S.-W. Chu. Nonlinear plasmonics at high temperatures. *Nanophotonics*, 317-328:6, 2017.
- [15] G. Baffou and H. Rigneault. Femtosecond-pulsed optical heating of gold nanoparticles. *Phys. Rev. B*, 84:035415, 2011.
- [16] G. Baffou and R. Quidant. Thermo-plasmonics: using metallic nanostructures as nano-sources of heat. *Laser Photon. Rev.*, 7:171–187, 2013.
- [17] P. R. West, S. Ishii, G. V. Naik, N. K. Emani, V. M. Shalaev, and A. Boltasseva. Searching for better plasmonic materials. *Laser Photon. Rev.*, 4:795–808, 2010.
- [18] F. Hache, D. Ricard, C. Flytzanis, and U. Kreibig. The optical Kerr effect in small metal particles and metal colloids: The case of gold. *Appl. Phys. A*, 47:347, 1988.
- [19] A. Lalis, G. Tessier, J. Plain, and G. Baffou. Quantifying the efficiency of plasmonic materials for near-field enhancement and photothermal conversion. *J. Phys. Chem. C*, 119:25518 – 25528, 2015.
- [20] X. Chen, A. Munjiza, K. Zhang, and D. Wen. Molecular dynamics simulation of heat transfer from a gold nanoparticle to a water pool. *J. Phys. Chem. C*, 118:1285 – 1293, 2014.
- [21] O. Neumann, A. S. Urban, J. Day, S. Lal, P. Nordlander, and N. J. Halas. Solar vapor generation enabled by nanoparticles. *ACS Nano*, 7:42–49, 2013.
- [22] Z. Fang, Y. R. Zhen, O. Neumann, A. Polman, F. J. Garcia de Abajo, P. Nordlander, and N. J. Halas. Evolution of light-induced vapor generation at a liquid-immersed metallic nanoparticle. *Nano Lett.*, 13:1736–1742, 2013.
- [23] G. Baffou, J. Polleux, H. Rigneault, and S. Monneret. Super-heating and micro-bubble generation around plasmonic nanoparticles under CW illumination. *J. Phys. Chem. C*, 118:4890–4898, 2014.
- [24] X. C. Li, J. M. Zhao, L. H. Liu, and J. Y. Tan. Optical properties of edible oils within spectral range from 300 to 2500nm determined by double optical pathlength transmission method. *Applied Optics*, 54:3886–3893, 2015.
- [25] S. Adachi. *Properties of AlGaAs*. IET, 1993.
- [26] I. Strzalkowski and S. Joshi and C.R. Crowell. Dielectric constant and its temperature dependence for GaAs, CdTe, and ZnSe. *Appl. Phys. Lett.*, 28:350, 1976.
- [27] M. Guerrisi, R. Rosei, and P. Winsemius. Splitting of the interband absorption edge in Au. *Phys. Rev. B*, 12:557–563, 1975.

- [28] P. Winsemius, M. Guerrisi, and R. Rosei. Splitting of the interband absorption edge in Au: Temperature dependence. *Phys. Rev. B*, 12:4570, 1975.
- [29] L. Sarkhosh and N. Mansour. Study of the solution thermal conductivity effect on nonlinear refraction of colloidal gold nanoparticles. *Laser Phys.*, 25:065404, 2015.
- [30] S. Sadat, A. Tan, Y. J. Chua, and P. Reddy. Nanoscale thermometry using point contact thermocouples. *Nano letters*, 10:2613–2617, 2010.
- [31] G. Kucsko, P. C. Maurer, N. Y. Yao, M. Kubo, H. J. Noh, P. K. Lo, H. Park, and M. D. Lukin. Nanometre-scale thermometry in a living cell. *Nature*, 500:54–58, 2013.
- [32] M. Mecklenburg, W. A. Hubbard, E. R. White, R. Dhall, S. B. Cronin, S. Aloni, and B. C. Regan. Nanoscale temperature mapping in operating microelectronic devices. *Science*, 347:629, 2015.
- [33] Y.-K. Tzeng, P.-C. Tsai, H.-Y. Liu, O. Y. Chen, H. Hsu, F.-G. Yee, M.-S. Chang, and H.-C. Chang. Time-resolved luminescence nanothermometry with nitrogen-vacancy centers in nanodiamonds. *Nano Lett.*, 15:3945–3952, 2015.
- [34] K. Kim, B. Song, V. Fernández-Hurtado, W. Lee, W. Jeong, L. Cui, D. Thompson, J. Feist, M. T. Homer Reid, F. J. García-Vidal, J. Carlos Cuevas, E. Meyhofer, and P. Reddy. Radiative heat transfer in the extreme near field. *Nature*, 528:387–391, 2015.
- [35] J. T. Hugall and J. J. Baumberg. Demonstrating photoluminescence from Au is electronic inelastic light scattering of a plasmonic metal: The origin of sers backgrounds. *Nano Lett.*, 15:2600–2604, 2015.
- [36] U. Gurudas, E. Brooks, D.M. Bubb, S. Heiroth, T. Lippert, and A. Wokaun. Saturable and reverse saturable absorption in silver nanodots at 532 nm using picosecond laser pulses. *J. Appl. Phys.*, 104:073107, 2008.
- [37] H.I. Elim, J. Yang, J.-Y. Lee, J. Mi, and W. Ji. Observation of saturable and reverse-saturable absorption at longitudinal surface plasmon resonance in gold nanorods. *Appl. Phys. Lett.*, 88:083107, 2006.
- [38] S. Dengler, C. Kübel, A. Schwenke, G. Ritt, and B. Eberle. Near- and off-resonant optical limiting properties of gold-silver alloy nanoparticles for intense nanosecond laser pulses. *J. Opt.*, 14:075203, 2012.
- [39] Note that  $\Delta T_{lin}^{on}$  scales with  $a^2$  because it is the ratio of the absorption within the volume,  $\sigma_{abs} \sim a^3$ , and the rate of heat transfer to the host, given by  $(\kappa_{h,0}/a)$  times the surface area

$a^2$  through which heat leaks to the host.

- [40] Accordingly, we adopt below the standard terminology of nonlinear optics, namely, the term proportional to  $I_{inc} \sim |E_{inc}|^2$  will be referred to as the cubic term and the term proportional to  $I_{inc}^2 \sim |E_{inc}|^4$  will be referred to as the quintic term.
- [41] Relative errors in the permittivity and field are of comparable magnitude.
- [42] i.e., a temperature increase of  $323^\circ K$  instead of  $300^\circ K$ . The corresponding errors in the permittivity and field are similar.
- [43] As noted below, this relation is fairly general, see Eq. (12).
- [44] Note that the expansion (11) is with respect to the *quadratic* solution, i.e., it is less accurate than the cubic-quintic fits to the *exact* solution shown in the plots of the nonlinear permittivities. Yet, in most cases, this gives a decent guidance regarding the relative importance of the various terms.
- [45] Eq. (12) enables one to simplify some of the coefficients in Eq. (4). However, as shown below regarding the quadratic approximation (10), this approach has only a limited accuracy.
- [46] As an aside, we note that a similar behaviour was seen in [18, Fig. 1] for dilute composites under *picosecond* illumination. However, there are also reports of a potentially opposite behaviour (e.g., [36–38]). This reflects the sensitivity of the problem to the illumination wavelength, scatterer size and for pulsed illumination, also for the duration of the illumination.
- [47] Such increased scattering was observed for ultrafast illumination, see e.g. [36–38], and was repeatedly interpreted as a saturable absorption; however, to the best of our knowledge, no conclusive proof regarding the origin of the effect was ever given.
- [48] We expect the shape to affect the cubic coefficient as well, however, a quantification of this effect requires more exact numerical calculations that we will perform only in a future study.
- [49] the latter effect may explain the rather surprising increase of scattering observed for high intensities that seem to dominate the thermal effect [5–8].